Analytical and numerical solution of the Schrödinger equation for a surface potential barrier including spin-orbit interaction

M. M. Moya and J. S. Helman

Citation: American Journal of Physics **47**, 452 (1979); doi: 10.1119/1.11815

View online: http://dx.doi.org/10.1119/1.11815

View Table of Contents: http://scitation.aip.org/content/aapt/journal/ajp/47/5?ver=pdfcov

Published by the American Association of Physics Teachers

Analytical and numerical solution of the Schrödinger equation for a surface potential barrier including spin-orbit interaction

M. M. Moya
Facultad de Física, Universidad de Veracruz, Jalapa, Veracruz, Mexico

J. S. Helman
Departamento de Física, Centro de Investigación del Instituto Politécnico Nacional, Apartado Postal 14-740, México 14, Distrito Federal, Mexico
(Received 17 May 1978; accepted 24 November 1978)

We consider the problem of an electron interacting with a surface potential barrier which includes the spin-orbit interaction. An exact solution of the Schrödinger equation is given for the case of a step potential. For smooth barrier profiles, the time- dependent Schrödinger equation is numerically solved, and the time evolution of the spin-up and spin-down components of a wave packet is displayed in a series of pictures.

I. INTRODUCTION

The spin-orbit (SO) interaction between an electron and the surface barrier of a metal has been studied in the past in order to estimate its effect on the conduction electron-spin relaxation.[1,2]

The analysis of the conduction electron-spin relaxation induced by the presence of clean and dirty surfaces is relevant for the interpretation of experimental results on polarized electron emission from magnetic materials,[3] on the Knight shift of small superconducting particles[4] and also on the conduction electron spin resonance linewidth of small normal metallic particles.[5,6]

Although estimates show that in most of the above mentioned cases the SO interaction plays a minor role, the problem is still interesting from a pedagogical point of view. The three-dimensional Schrödinger equation can be exactly solved for the case of a step potential surface barrier (Sec. III) and, in the case of a barrier with arbitrary profile, the numerical solution of the time-dependent Schrödinger equation allows to visualize the time evolution of an electron wave packet with both spin-up and spin-down components as it strikes the barrier (Sec. IV).

The results of the computation are shown in Sec. VI.

II. MODEL

Let us consider a semi-infinite metal. The metal is described by a Sommerfeld model, that is, a free-electron gas of density n (electrons per cm^3) with a surface potential barrier given by

$$V(z) = -V_0/(e^{z/a}+1). \tag{1}$$

The coordinate system is chosen with the z direction perpendicular to the surface of the metal. The step potential barrier corresponds to the limit $a \to 0$. $k_F = (3\pi^2 n)^{1/3}$ is the Fermi momentum and $E_F = \hbar^2 k_F/2m$ is the Fermi energy. $\phi = V_0 - E_F$ is the work function of the metal. m is the free-electron mass and $\hbar$ is Planck's constant.

We consider the Hamiltonian[7]

$$H = -(\hbar^2/2m)\nabla^2 + V(z) + (1/2m^2c^2)\mathbf{s}\times\mathbf{p}\cdot\nabla V(z). \tag{2}$$

Here $\mathbf{s}$ and $\mathbf{p}$ are the spin and momentum electron operators, c is the velocity of light in vacuum, and ∇ denotes the gradient operator. The spin quantization axis is chosen along the z direction. The first term describes the electron kinetic energy, the second term is the surface potential and the third term represents the SO interaction responsible for the finite probability of spin flip when the electron strikes the barrier.

Since $V(z)$ has translational invariance in any direction perpendicular to the z axis, the x and y components of the wave vector $\mathbf{k} = \mathbf{p}/\hbar$ are constants of the motion.

Thus, the eigenfunctions of H are spinors of the form

$$\phi(x,y,z) = \chi(z)e^{i(k_x x + k_y y)}. \tag{3}$$

With the wave function (3), the three-dimensional Schrödinger equation

$$H\phi = E\phi, \tag{4}$$

reduces to the following one-dimensional Schrödinger equation for $\chi(z)$,

$$H_1\chi(z) = \epsilon\chi(z), \tag{5}$$

where

$$H_1 = -\frac{\hbar^2}{2m}\frac{d^2}{dz^2} + V(z) + \frac{\hbar^2}{4m^2c^2}\frac{dV(z)}{dz}(\sigma_x k_y - \sigma_y k_x) \tag{6}$$

and $\epsilon = E - \hbar^2 k_t^2/2m$ with $k_t^2 = k_x^2 + k_y^2$. In writing Eq. (5) we used the Pauli matrix representation for the spin operator $\mathbf{s} = (\hbar/2)\boldsymbol{\sigma}$.[8]

In general, the system of differential equations (5) cannot be solved analytically in a closed form. However, for a step potential ($a \to 0$), there is an exact solution as it is shown in Sec. III.

The three-dimensional time-dependent Schrödinger equation corresponding to this model is

$$H\phi(x,y,z,t) = i\hbar\frac{\partial\phi(x,y,z,t)}{\partial t}. \tag{7}$$

Using a wave function of the form

$$\phi(x,y,z,t) = \psi(z,t)e^{i(k_x x + k_y y) - i[(E-\epsilon)/\hbar]t}, \tag{8}$$

 0002-9505/79/050452-05$00.50

Eq. (7) reduces to a one-dimensional time-dependent Schrödinger equation, whose formal solution can be written

$$\psi(z,t) = e^{-i(H_1/\hbar)(t-t_0)}\psi(z,t_0). \tag{9}$$

To calculate numerically the time evolution of $\psi(z,t)$ we consider the metal and the vacuum contained in a quantization box of rigid walls, of length $L \gg a$.

III. EXACT SOLUTION FOR A STEP BARRIER

In the limit $a \to 0$, Eq. (1) becomes

$$V(z) = -V_0\theta(-z), \tag{10}$$

where $\theta(z) = 1$ for $z > 0$ and $\theta(z) = 0$ for $z < 0$. Thus,

$$\frac{dV}{dz} = V_0\delta(z), \tag{11}$$

where $\delta(z)$ is Dirac's δ function. Equation (5) becomes

$$-\frac{\hbar^2}{2m}\frac{d^2\chi(z)}{dz^2} - V_0\theta(-z)\chi(z) + \frac{\hbar^2 A}{2m}\delta(z)\begin{pmatrix}0 & k^+\\ k^- & 0\end{pmatrix}\chi(z) = \epsilon\chi(z) \tag{12}$$

where $k^{\pm} = k_y \pm ik_x$, and $A = V_0/2mc^2$.

For $\epsilon > 0$ we try the solution

$$\chi(z) = \begin{pmatrix}e^{iKz} + r_\uparrow e^{-iKz}\\ r_\downarrow e^{-iKz}\end{pmatrix}, \tag{13}$$

for $z < 0$ and

$$\chi(z) = \begin{pmatrix}t_\uparrow e^{ikz}\\ t_\downarrow e^{ikz}\end{pmatrix}, \tag{14}$$

for $z > 0$, where

$$K^2 = (2m/\hbar^2)(\epsilon + V_0),$$
$$k^2 = (2m/\hbar^2)\epsilon. \tag{15}$$

This solution corresponds to a plane wave with spin up ("up" means in the positive z direction) coming from the bulk of the metal with amplitude one, which is partially reflected at the surface with spin up (amplitude $r_\uparrow$) and spin down (amplitude $r_\downarrow$) and partially transmitted to vacuum with spin up (amplitude $t_\uparrow$) and spin down (amplitude $t_\downarrow$).

The continuity condition on $\chi(z)$ at $z = 0$ requires that

$$1 + r_\uparrow = t_\uparrow,\ r_\downarrow = t_\downarrow. \tag{16}$$

Furthermore, due to the presence of the δ function in Eq. (5), it is required that the derivatives $\chi'(0^+)$, $\chi'(0^-)$ and the function $\chi(0)$ satisfy the relation[9]

$$\chi'(+0) - \chi'(-0) = A^2\begin{pmatrix}0 & k^+\\ k^- & 0\end{pmatrix}\chi(0), \tag{17}$$

which leads to the additional conditions

$$\begin{aligned} ikt_\uparrow + iKr_\uparrow - iK &= Ak^+t_\downarrow\\ ikt_\downarrow + iKr_\downarrow &= Ak^-t_\uparrow. \end{aligned} \tag{18}$$

From Eqs. (16) and (18) we obtain

$$\begin{aligned} t_\uparrow &= 1 + r_\uparrow = 2K(k+K)/\Delta,\\ t_\downarrow &= r_\downarrow = -2KAk^+/\Delta, \end{aligned} \tag{19}$$

where $\Delta = (k+K)^2 + A^2k_t^2$. The corresponding reflection and transmission coefficients are

$$R_\uparrow = |r_\uparrow|^2 = [(K^2 - k^2 - A^2k_t^2)/\Delta]^2,$$
$$T_\uparrow = |t_\uparrow|^2 = 4K^2(k+K)^2/\Delta^2$$
$$R_\downarrow = T_\downarrow = |r_\downarrow|^2 = |t_\downarrow|^2 = 4K^2A^2k_t^2/\Delta^2. \tag{20}$$

It is noteworthy that the corrections introduced by the spin-orbit interaction are of the order of A^2 for $A \ll 1$ (as it is the case in metals).

For $\epsilon < 0$, the electron is totally reflected by the barrier. Equations (19) and (20) are still valid if we replace k by ik' where $k' = -(2m/\hbar)^{1/2}\epsilon$. In this case we obtain

$$R'_\uparrow = (K^2 + k'^2 - A^2k_t^2)^2/|\Delta'|^2,$$
$$T'_\uparrow = 4K^2(K^2 + k'^2)/|\Delta'|^2,$$
$$R'_\downarrow = T'_\downarrow = 4K^2A^2k_t^2/|\Delta'|^2, \tag{21}$$

where $|\Delta'|^2 = (K^2 - k'^2 + A^2k_t^2)^2 + 4K^2k'^2$. Note that $R'_\uparrow + R'_\downarrow = 1$ and $K^2 + k'^2 = (2m/\hbar^2)V_0$. Up to order A^2 we obtain

$$R'_\downarrow = [K^2k_t^2/(mc^2)^2](\hbar^2/2m)^2, \tag{22}$$

which is independent of V_0.

For an electron on the Fermi surface is $k_t^2 = k_F^2 - K^2$. If we write $K = k_F\cos\theta$ and make an average over $\cos\theta$ between 0 and 1 (because only the electrons moving towards the surface have to be considered) we obtain

$$R'_\downarrow = (2/15)(E_F/mc^2)^2. \tag{23}$$

This value was previously derived by Lisin *et al.*,[1] who showed in a very elegant way that in the first Born approximation the value of $R'_\downarrow$ (which they call ϵ_0) is independent of the profile chosen for $V(z)$.

IV. NUMERICAL CALCULATION

To solve numerically Eq. (9) we use the technique of Goldberg *et al.*,[10] generalized to include the spin-orbit interaction. The Hamiltonian (6) can be written in the form

$$H_1 = -\frac{\hbar^2}{2m}\frac{d^2}{dz^2} + V(z) + \frac{\hbar^2}{4m^2c^2}\frac{dV(z)}{dz}\hat{K}, \tag{24}$$

where $\hat{K}$ is the matrix

$$\hat{K} = \begin{pmatrix}0 & k^+\\ k^- & 0\end{pmatrix} \tag{25}$$

and we shall denote the spinor $\psi(z,t)$ by

$$\psi(z,t) = \begin{pmatrix}\phi_\uparrow(z,t)\\ \phi_\downarrow(z,t)\end{pmatrix}, \tag{26}$$

where $\phi_\uparrow(z,t)$ is the amplitude of probability for an electron with spin up and, analogously, $\phi_\downarrow(z,t)$ for spin down.

For the numerical calculation we use the following discrete functions:

$$\psi(z,t) \to \psi_j^n,\ V(z) \to V_j,\ \frac{dV(z)}{dz} \to \xi_j. \tag{27}$$

$t = \delta n$ and $z = \epsilon' j$ where δ and ϵ' are appropriate intervals of time and space, respectively, and n and j are integers. j

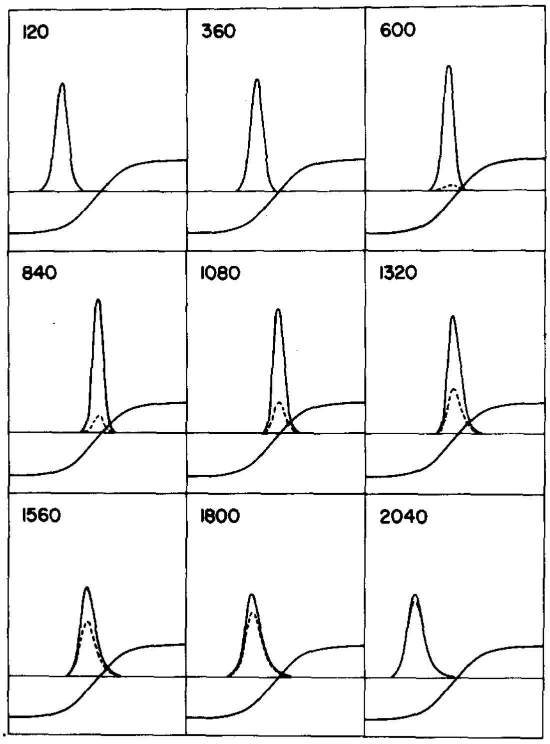

Fig. 1. Time evolution of a wave packet with $k = 1.0 \times 10^8$ cm^{-1} in a potential barrier with $a = 12.5 \times 10^{-8}$ cm. The full line represents the spin up component and the dotted line represents the spin down component enlarged by a factor 0.8×10^{11}.

runs from 0 to J, where $J = L/\epsilon'$ and n runs from 0 up to a value large enough so that the wave packet reaches and leaves the barrier.

Using Caley approximation

$$e\frac{-iH_1\delta}{\hbar} \simeq \frac{1 - i\delta H_1/2\hbar}{1 + i\delta H_1/2\hbar}, \tag{28}$$

and following the algebra of Ref. 10 we obtain the following discrete form for Eq. (9):

$$\psi_{j+1}^{n+1} + (\Gamma V_j + i\lambda - 2)\psi_j^{n+1} + \psi_{j-1}^{n+1} - \rho\xi_j\hat{K}\psi_j^{n+1} = \Omega_j^n + \rho\xi_j\hat{K}\psi_j^n, \tag{29}$$

where $\lambda = 4m\epsilon'^2/\delta\hbar$, $\rho = \epsilon'^2/2mc^{2\prime}$, $\Gamma = 2m\epsilon'^2/\hbar^2$, and

$$\Omega_j^n = -\psi_{j+1}^n + (2 - \Gamma V_j + i\lambda)\psi_j^n - \psi_{j-1}^n. \tag{30}$$

Assuming it is possible to write an iterative expression of the form

$$\psi_{j+1}^{n+1} = \hat{e}_j\psi_j^{n+1} + f_j^n, \tag{31}$$

where the matrix $\hat{e}_j$ and the spinor f_j^n are defined by Eq. (31), then Eq. (29) becomes

$$\psi_j^{n+1} = [(\Gamma V_j + i\lambda - 2) + \hat{e}_j - \rho\xi_j\hat{K}]^{-1} \times [-\psi_{j-1}^{n+1} + (\Omega_j^n - f_j^n + \rho\xi_j\hat{K}\psi_j^n)]. \tag{32}$$

Comparing (32) with (31) we recognize that

$$\hat{e}_{j-1} = (\Gamma V_j + i\lambda - 2 + \hat{e}_j - \rho\xi_j\hat{K})^{-1} \tag{33}$$

and

$$f_{j-1}^n = -\hat{e}_{j-1}(\Omega_j^n + \rho\xi_j\hat{K}\psi_j^n - f_j^n),$$

from which we obtain the following iterative equations for $\hat{e}$ and f:

$$\hat{e}_j = 2 - \Gamma V_j - i\lambda - (\hat{e}_{j-1})^{-1} + \rho\xi_j\hat{K},$$
$$f_j^n = \Omega_j^n + \rho\xi_j\hat{K}\psi_j^n + \hat{e}_{j-1}f_{j-1}^n. \tag{34}$$

Writing $j = 1$ in Eq. (29) and comparing with Eq. (31) for $j = 1$ we obtain

$$\hat{e}_1 = 2 - \Gamma V_j - i\lambda + \rho\xi_1\hat{K},\ f_1^n = \Omega_1^n + \rho\xi_1\hat{K}\psi_1^n. \tag{35}$$

Writing $j = J - 1$ in Eq. (31) we obtain

$$\psi_{J-1}^{n+1} = -(\hat{e}_{J-1})^{-1}f_{J-1}^n, \tag{36}$$

which is a particular case which results of inverting Eq. (31), namely

$$\psi_j^{n+1} = (\hat{e}_j)^{-1}(\psi_{j+1}^{n+1} - f_j^n). \tag{37}$$

Thus, given the initial wave packet ψ_j^0, from Eq. (30) we know Ω_j^0 and from Eqs. (34) and (35) we obtain f_j^0. Then Eq. (36) gives the value of ψ_{J-1}^1 and by iteration Eq. (37) gives ψ_j^1. Continuing the iteration we obtain ψ_j^n for all j and n.

V. NUMERICAL PARAMETERS

The numerical values of the parameters used in the calculation were the following: $m = 0.91 \times 10^{-27}$ g, $\hbar = 1.05 \times 10^{-27}$ erg sec, $V_0 = 12.5 \times 10^{-12}$ erg (=7.8 eV), $k_x = k_y = 1.0 \times 10^8$ cm^{-1}, $L = 1.57 \times 10^{-6}$ cm, $\delta = 5.554 \times 10^{-18}$ sec, and $\epsilon' = 1.57 \times 10^{-9}$ cm. The calculations were performed for two barrier profiles with $a = 3.0 \times 10^{-8}$ cm and 12.5×10^{-8} cm. The initial wave packet is the normalized Gaussian curve

$$\psi(z, 0) = \frac{e^{ikz}e^{-(z-z_0)^2/2\sigma_0^2}}{[\sigma_0(\pi)^{1/2}]^{1/2}}\begin{pmatrix}1\\0\end{pmatrix}, \tag{38}$$

with $z_0 = L/4$ and $\sigma_0 = 7.85 \times 10^{-8}$ cm. The calculations

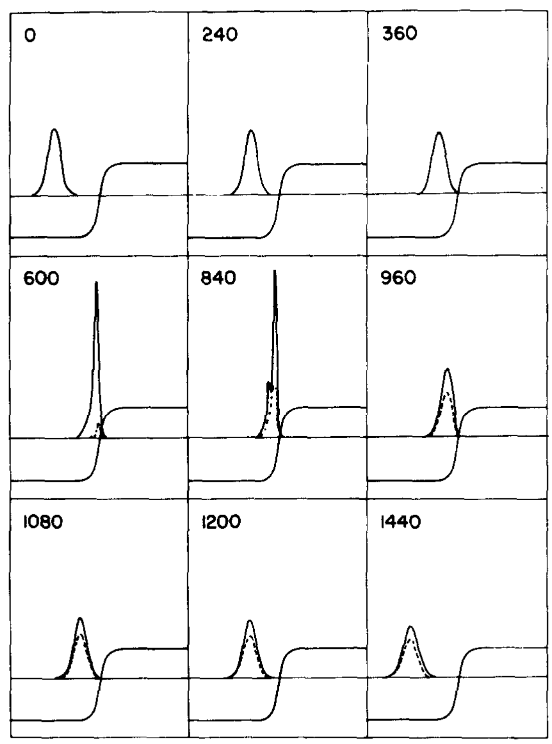

Fig. 2. Time evolution of a wave packet with $k = 1.0 \times 10^8$ cm^{-1} in a potential barrier with $a = 3.0 \times 10^{-8}$ cm. The full line represents the spin-up component and the dotted line represents the spin-down component enlarged by a factor 0.715×10^{11}.

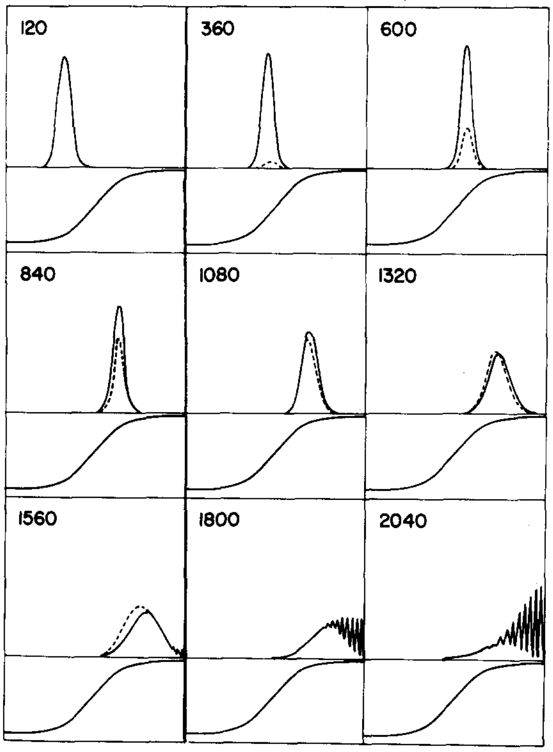

Fig. 3. Time evolution of a wave packet with $k = 1.423 \times 10^8$ cm^{-1} in a potential barrier with $a = 12.5 \times 10^{-8}$ cm. The full line represents the spin up component and the dotted line represents the spin-down component enlarged by a factor 0.8×10^{11}.

were made for two values of k: $k = 1.0 \times 10^8$ cm^{-1} (corresponding to $\epsilon = 3.79$ eV) and $k = 1.423 \times 10^8$ cm^{-1} (corresponding to $\epsilon = 7.9$ eV). These parameters satisfy the convergence requirements pointed out in Ref. 10.

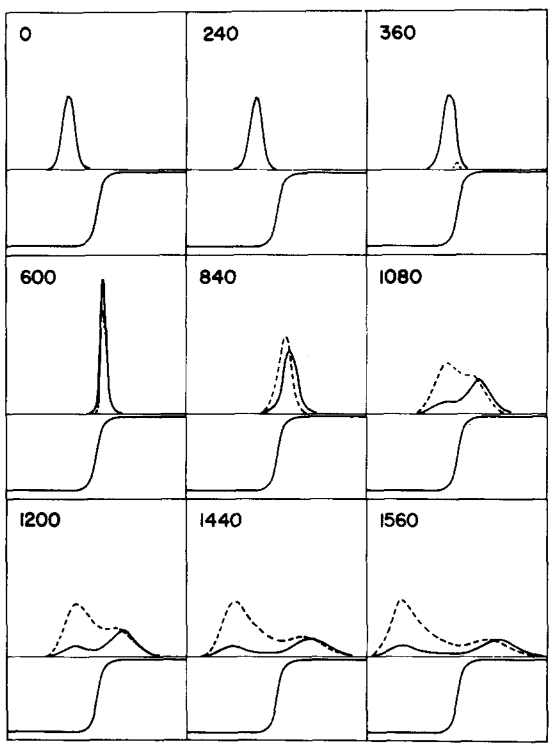

Fig. 4. Time evolution of a wave packet with $k = 1.423 \times 10^8$ cm^{-1} in a potential barrier with $a = 3.0 \times 10^{-8}$ cm. The full line represents the spin-up component and the dotted line represents the spin-down component enlarged by a factor 0.66×10^{11}.

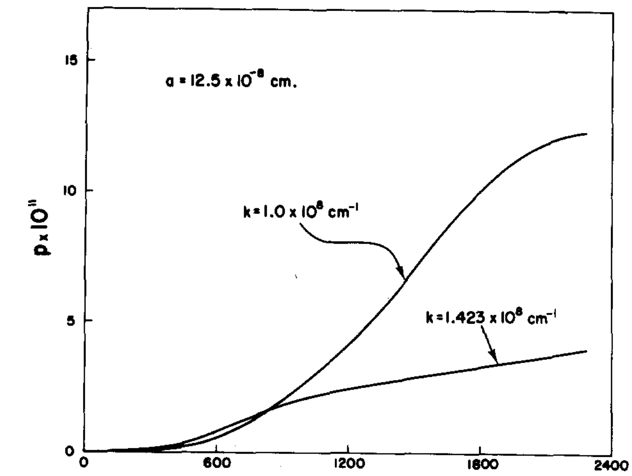

Fig. 5. Probability P that the wave packet in a barrier with $a = 12.5 \times 10^{-8}$ cm is found with spin down at time t for $k = 1.0 \times 10^8$ cm^{-1} and $k = 1.423 \times 10^8$ cm^{-1}.

VI. RESULTS AND DISCUSSION

The time evolution of the wave packets $|\phi_\uparrow(z,t)|^2$ (full line) and $|\phi_\downarrow(z,t)|^2$ (dotted line) for different energies (ϵ) and barrier profiles (a) is shown in Figs. 1–4. In the graphs the scale of the probability density for spin down, $|\phi_\downarrow(z,t)|^2$ has been enlarged by the factors 0.8×10^{11}, 0.715×10^{11}, 0.8×10^{11}, and 0.66×10^{11} in Figs. 1–4, respectively, for the sake of clarity in the display. The numbers in the upper left corners of each square of Figs. 1–4 denote the time in units of δ. The base line of the wave packet corresponds to its energy referred to the potential. Figure 1 corresponds to a wave packet with $k = 1.0 \times 10^8$ cm^{-1} in a potential barrier with $a = 12.5 \times 10^{-8}$ cm, and Fig. 2 corresponds to the same wave packet in a barrier with $a = 3.0 \times 10^{-8}$ cm. Analogously, Figs. 3 and 4 correspond to a wave packet with $k = 1.423 \times 10^8$ cm^{-1} in barrier with $a = 12.5 \times 10^{-8}$ cm and $a = 3.0 \times 10^{-8}$ cm, respectively.

When $k = 1.0 \times 10^8$ cm^{-1} ($\epsilon < V_0$), the wave packet with spin-up strikes the barrier and is reflected with spin-up and spin-down components. When $k = 1.423 \times 10^8$ cm^{-1} ($\epsilon > V_0$), the wave packet with spin up is partially reflected and partially transmitted with spin-up and spin-down components. The build up of the spin-down component during the time evolution of the wave packet can be followed in Figs. 1–4.

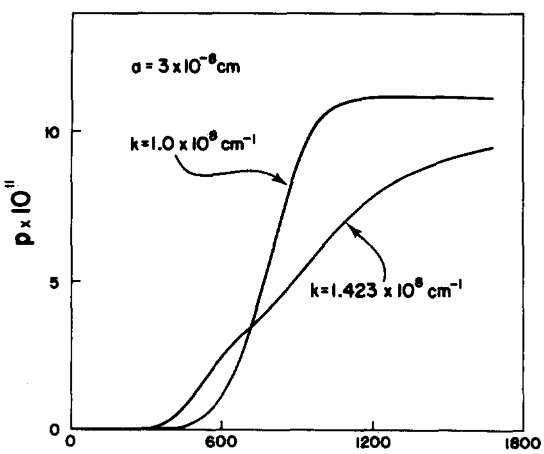

Fig. 6. Probability P that the wave packet in a barrier with $a = 3.0 \times 10^{-8}$ cm is found with spin down at time t for $k = 1.0 \times 10^8$ cm^{-1} and $k = 1.423 \times 10^8$ cm^{-1}.

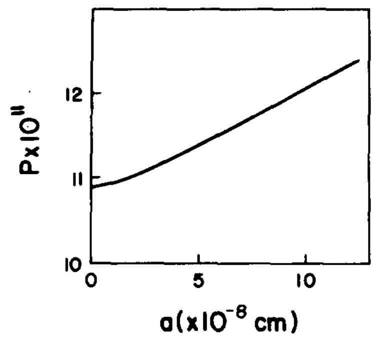

Fig. 7. Spin-flip probability in reflexion, $P(\infty)$, as a function of the barrier parameter a (see remarks in the text).

The strong oscillation of the wave packet in Fig. 3 for $t \gtrsim 1560\delta$ is a spurius consequence of its interaction with the rigid wall of the quantization box. In Fig. 3, the reflected part of the wave packet is not apparent because, due to the smoothness of the potential, the reflexion coefficient is small.

The probability that the wave packet is found with spin down at time t,

$$P(t) = \int_{-\infty}^{\infty} |\phi_{\downarrow}(z,t)|^2 \, dz$$

is plotted as a function of t, for the four cases considered above, in Figs. 5 and 6. Within our computation times, saturation was clearly observed in only one case: $k = 1.0 \times 10^8 \text{ cm}^{-1}$, $a = 3.0 \times 10^{-8}$ cm.

In Fig. 7 we plotted $P(\infty)$ for $k = 1.0 \times 10^8 \text{ cm}^{-1}$ as a function of a. The curve is an interpolation between the points corresponding to $a = 0$ [exact result, Eq. (21)], $a = 3.0 \times 10^{-8}$ cm (numerical result taken from Fig. 6), and $a = 12.5 \times 10^{-8}$ cm (numerical result extrapolated from Fig. 5). Within the first Born approximation, which is extremely accurate for this problem, $P(\infty)$ is independent of the barrier profile.[1] Since we find a change of 10% in $P(\infty)$ for a in the range $0\text{–}12.5 \times 10^{-8}$ cm, this change must be attributed to the accumulation of numerical errors.

We are in the process of generating a motion picture showing the time evolution of the wave packets under the different conditions considered in this paper.

ACKNOWLEDGMENTS

We thank the Centro de Procesamiento y Evaluación of the Secretaría de Educación Pública for allowing us the use of their computational facilities (Univac 1106). This work was partially supported by Consejo Nacional de Ciencia y Tecnología (Mexico).

[1]V. N. Lisin and B. M. Khabibullin, Sov. Phys. Solid State **17**, 1045 (1975) [Fiz. Tverd. Tela. **17**, 1598 (1975)].

[2]J. S. Helman and F. Sánchez-Sinencio, Bol. Soc. Mexicana Fís. **4** (1974).

[3]J. S. Helman and H. C. Siegmann, Solid State Commun. **13**, 891 (1973).

[4]D. E. MacLaughlin, Solid State Phys. **31**, 1 (1976).

[5]S. K. Wang and R. T. Schumacher, Phys. Rev. B **8**, 4119 (1973); **10**, 2129 (1974).

[6]M. A. Smithard, Solid State Commun. **14**, 411 (1974).

[7]E. Merzbacher, *Quantum Mechanics* (Wiley, New York, 1970), p. 433.

[8]Reference 7, p. 270.

[9]I. I. Gol'dman and V. D. Kirvchenkov, *Problems in Quantum Mechanics* (Pergamon, London, 1961), p. 9.

[10]A. Goldberg, H. M. Schey, and J. L. Schwartz, Am. J. Phys. **35**, 177 (1967).